Deterministic Squeezed States with Collective Measurements and Feedback

Kevin C. Cox, Graham P. Greve, Joshua M. Weiner, and James K. Thompson
JILA, NIST, and University of Colorado, 440 UCB, Boulder, Colorado 80309, USA
(Received 7 December 2015; published 4 March 2016)

We demonstrate the creation of entangled, spin-squeezed states using a collective, or joint, measurement and real-time feedback. The pseudospin state of an ensemble of $N = 5 \times 10^4$ laser-cooled ^{87}Rb atoms is deterministically driven to a specified population state with angular resolution that is a factor of 5.5(8) [7.4 (6) dB] in variance below the standard quantum limit for unentangled atoms—comparable to the best enhancements using only unitary evolution. Without feedback, conditioning on the outcome of the joint premeasurement, we directly observe up to 59(8) times [17.7(6) dB] improvement in quantum phase variance relative to the standard quantum limit for $N = 4 \times 10^5$ atoms. This is one of the largest reported entanglement enhancements to date in any system.

DOI: 10.1103/PhysRevLett.116.093602

Entanglement is a fundamental quantum resource, able to improve precision measurements and required for all quantum information science. Advances in the creation, manipulation, and characterization of entanglement will be required to develop practical quantum computers, quantum simulators, and enhanced quantum sensors. In particular, quantum sensors operate by attempting to estimate the total amount of phase that accumulates between two quantum states, typically forming a pseudospin-1/2. When N atoms are unentangled, the independent quantum projection or collapse of each atom's wave function fundamentally limits the sensor by creating a rms uncertainty $\Delta\theta_{\mathrm{SQL}} = 1/\sqrt{N}$ rad in the estimate of the quantum phase, the standard quantum limit (SQL) [1]. However, entanglement can be used to create correlations in the quantum collapse of the N atoms [2,3] to achieve large enhancements in phase resolution, in principle down to the Heisenberg limit $\Delta\theta_{\mathrm{HL}} = 1/N$ rad.

This Letter features two main results. First, following Fig. 1(a), we use the outcome of a collective, or joint, measurement to actively steer the collective spin projection of an ensemble of 5×10^4 laser-cooled and trapped ^{87}Rb atoms to a target entangled quantum state. Real-time feedback allows generation of the target state with enhanced angular resolution $S^{-1} \equiv (\Delta\theta_{\mathrm{SQL}}/\Delta\theta)^2 = 5.5(8)$, or 7.4(6) dB below the SQL, with no background subtractions. Second, we perform a direct subtraction of quantum noise without feedback and directly observe a conditionally enhanced phase resolution $S^{-1} = 59(8)$ or equivalently 17.7(6) dB below the SQL. Along with another recent result using similar collective measurements [4], this is the largest phase enhancement from entanglement to date in any system.

Entanglement is often created and manipulated via unitary interactions between qubits [9–18]. However, the joint measurements on two or more qubits used here (sometimes referred to as quantum nondemolition measurements) have shown promise for creating entanglement, particularly among large numbers of qubits [19–30]. By adding real-time feedback guided by the outcome of joint measurements, one can access a more diverse range of quantum technologies including Heisenberg-limited atomic sensors [31], reduction of mean field shifts in atom interferometers [32,33], quantum teleportation [34,35], and error correction [36,37]. Quantum noise suppression

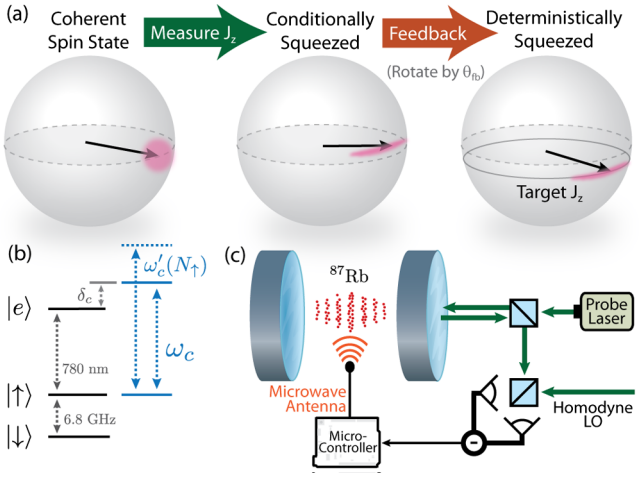

FIG. 1. (a) A coherent spin state's spin-projection noise (pink distribution) is projected onto a squeezed state by a measurement of J_z. The quantum state randomly collapses within the original distribution, creating a conditionally squeezed state. The premeasurement's outcome is then used to rotate the spin state's polar angle to a desired target spin projection (black solid line) $J_z = J_{z\mathrm{tar}}$, creating a deterministically squeezed state. (b) The relevant ^{87}Rb energy levels (black) and cavity resonance frequency ω_c (blue). (c) Simplified experimental diagram. The cavity is probed in reflection. Homodyne detection of the probe is sampled by a microcontroller that then applies microwaves at 6.8 GHz to achieve the desired feedback rotation θ_{fb} to create the deterministically squeezed state in (a). See the Supplemental Material [5] for experimental details.

 © 2016 American Physical Society

with real-time feedback has been considered theoretically [38,39] and demonstrated in a previous experiment [40] but without the critical enhancement in phase resolution that signifies entanglement.

We visualize a collection of N spin-1/2 atoms as a single collective Bloch vector $\mathbf{J} = J_x\hat{x} + J_y\hat{y} + J_z\hat{z}$ given by first order expectation values $J_\alpha \equiv \langle \hat{J}_\alpha \rangle$ of collective spin projection operators with $\alpha = \{x, y, z\}$. The quantum projection noise (QPN) and resulting SQL can be intuitively visualized by a quasiprobability distribution perpendicular to the classical Bloch vector [Fig. 1(a)]. The distribution's rms fluctuations along a given spin-projection direction are given by $\Delta J_\alpha \equiv \sqrt{\langle \hat{J}_\alpha^2 \rangle - \langle \hat{J}_\alpha \rangle^2}$. In this Letter Δ will refer to the standard deviation of a given quantity. For a coherent spin state oriented at the equator of the Bloch sphere, the spin projection J_z and spin population $N_\downarrow$ both fluctuate from one trial to the next with a standard deviation $\Delta J_{z,\mathrm{QPN}} = \Delta N_{\downarrow \mathrm{QPN}} \equiv \sqrt{N}/2$.

We calculate the enhancement in phase resolution $S \equiv (\Delta\theta/\Delta\theta_{\mathrm{SQL}})^2 = R/C^2$ [2], where $R \equiv (\Delta J_z/\Delta J_{z,\mathrm{QPN}})^2$ is the observed spin projection noise relative to the projection noise level, and $C \equiv 2\langle|\hat{J}|\rangle/N$ is the fractional atomic coherence remaining (or "contrast") after a joint measurement. An additional 0.2 dB correction is applied to S for a 4% background loss of contrast (see the Supplemental Material [5]). Observing $S^{-1} > 1$ serves as a witness for entanglement between atoms [41] and the magnitude usefully quantifies the degree of entanglement [2,3].

A joint measurement of the population of atoms $N_\uparrow$ is engineered by measuring the frequency shift of a TEM_{00} cavity mode. The cavity is tuned ($\delta_c = 2\pi \times 400$ MHz) to the blue of the ^{87}Rb $|\uparrow\rangle \equiv |5^2S_{1/2}, F = 2, M_F = 2\rangle$ to $|e\rangle \equiv |5^2P_{3/2}, F = 3, M_F = 3\rangle$ optical atomic transition as shown in Fig. 1(b). The second state forming the pseudospin system is $|\downarrow\rangle \equiv |5^2S_{1/2}, F = 1, M_F = 1\rangle$. The cavity has finesse 2532(80) and power decay linewidth $\kappa = 2\pi \times 3.15(10)$ MHz. The atoms are laser cooled to 10 μK and trapped tightly on axis in an intracavity 1D optical lattice [Fig. 1(c)]. Spatially inhomogeneous coupling of atoms to the cavity mode is handled as in Refs. [24,25,42,43]. Atoms in $|\uparrow\rangle$ strongly phase shift the intracavity probe light, causing the empty cavity resonance frequency ω_c to shift to ω_c'. A measurement of the shift $\omega_c' - \omega_c$ using homodyne detection of probe light reflected from the cavity can then be used to infer the population $N_\uparrow$. To measure the population $N_\downarrow$, a π-pulse microwave coupling can then be applied to swap the populations between $|\uparrow\rangle$ and $|\downarrow\rangle$, and a measurement of the new population in $|\uparrow\rangle$ can be made with the measurement outcome now labeled $N_\downarrow$.

The experimental sequence is shown in Figs. 2(a) and 2(b). All atoms are prepared in $|\downarrow\rangle$, then a microwave $\pi/2$ pulse is applied to place each atom in an equal superposition of spin states, equivalent to preparing the Bloch vector along

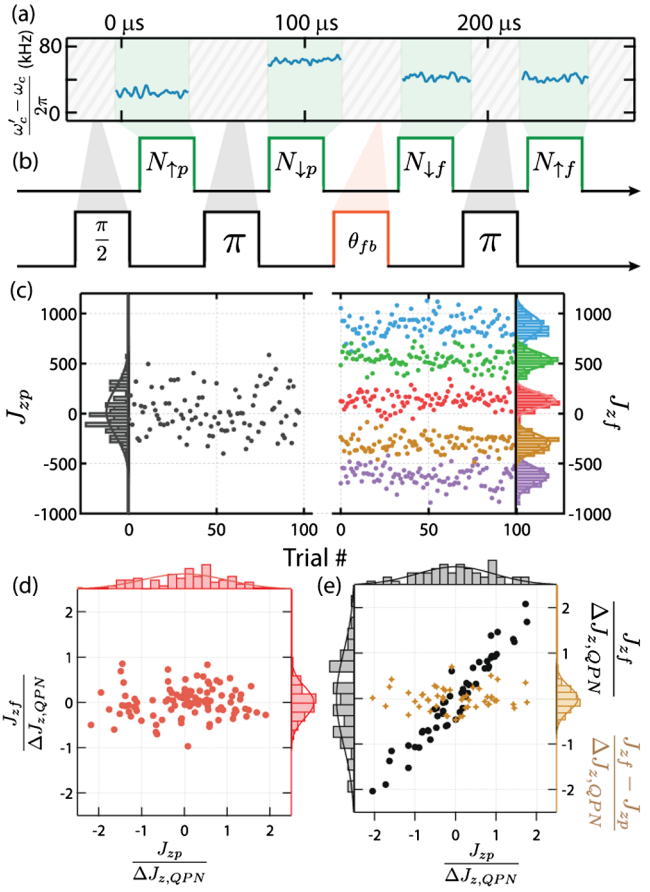

FIG. 2. (a) Measured cavity resonance frequency for a single trial versus time, subtracting a constant 12 MHz frequency offset. (b) The time windows in which the probe is turned on (green) and the populations determined from each window. The fixed microwave rotations are shown in black with the feedback rotation shown in orange. (c) The premeasurements J_{zp} (left) and final measurements J_{zf} (right) of J_z are plotted versus trial number and accumulated into histograms. Five different J_z states are targeted (five distinct colors on the right) and reached with noise below the QPN. The maximum deterministic squeezing is $S = -7.4(6)$ dB relative to the SQL. (d) Feedback reduces the noise distribution of the final measurement relative to the initial quantum noise in the premeasurement. (e) If no feedback is applied the final measurement and premeasurement are strongly correlated (black), allowing for conditional squeezing [$S = -10.3(6)$ dB] by using the differential quantity $J_{zf} - J_{zp}$ (gold). The increase in noise from feedback is discussed in the Supplemental Material [5].

$\hat{y}$. We make a measurement of the spin projection J_z with measurement outcome labeled $J_{zp} = (N_{\uparrow p} - N_{\downarrow p})/2$. Each population measurement outcome $N_{\uparrow p}$ and $N_{\downarrow p}$ is obtained by averaging the cavity-probe signal over a 40 μs window. In each run of the experiment, a microcontroller calculates J_{zp} and applies feedback to steer the state toward a targeted value of spin projection $J_{z\mathrm{tar}}$. The feedback is accomplished by applying microwaves to rotate the Bloch vector through polar angle $\theta_{\mathrm{fb}} \approx 2 \times (J_{z\mathrm{tar}} - J_{zp})/(NC)$. After the feedback, a final measurement of the spin projection J_z is made with measurement outcome labeled $J_{zf} = (N_{\uparrow f} - N_{\downarrow f})/2$.

Feedback toward $J_{zf} = 0$ is evident in the time trace [Fig. 2(a)], since the final two cavity frequency measurement windows that provide $N_{\uparrow f}$ and $N_{\downarrow f}$ are more nearly equal than was the case for the two premeasurement windows.

The microcontroller sets the sign of the rotation θ_{fb} by digitally toggling between two microwave sources that are 180° out of phase. The magnitude of the rotation $|\theta_{\mathrm{fb}}|$ is controlled by varying the duration t_{fb} for which the microwaves are applied, with a discrete timing resolution of approximately 12 ns. The input technical noise floor, timing jitter, and timing resolution of the microcontroller are all sufficient to allow up to 20 dB of squeezing.

The outcomes J_{zp} and J_{zf} are plotted versus trial number and collated into histograms in Fig. 2(c). Projection noise for these data (independently confirmed by measuring the scaling of ΔJ_z with N) is $\Delta J_{z,\mathrm{QPN}} = 218(10)$, consistent with the measured $\Delta J_{zp} = 235(24)$. The data on the right show the final measurement outcomes J_{zf} after applying feedback for five different target states $J_{z\mathrm{tar}}$. By implementing the feedback, each target state was reached with noise below the original projection noise.

To observe deterministic squeezing or phase resolution enhancement, the atomic coherence that remains after the premeasurement and feedback must be evaluated. The contrast is determined in a separate set of experiments by using microwave rotations after the feedback step to rotate the Bloch vector to determine its total length. Accounting for the loss of coherence, we directly observe up to $S^{-1} = 5.5(8)$ [7.4(6) dB] of deterministic squeezing via premeasurement and feedback.

For some applications, the feedback may not be necessary. Instead of applying feedback, one can cancel the quantum noise by directly subtracting the premeasurement J_{zp} from the final measurement J_{zf}, a technique known as conditional squeezing [19–27]. In Figs. 2(d) and 2(e), we compare conditional and deterministic spin noise reductions taken under identical settings. J_{zf} is plotted versus J_{zp} and the results are collated into histograms on each axis. With feedback (red), J_{zf} is driven to zero with resolution below $\Delta J_{z,\mathrm{QPN}}$, regardless of J_{zp}. Without feedback (black), J_{zp} and J_{zf} are correlated, and the quantum noise can be conditionally subtracted from the final measurement by taking the difference $J_{zf} - J_{zp}$ (gold).

The deterministic squeezing with feedback is primarily limited by errors in the π pulses due to microwave amplitude and frequency noise. However, by increasing the number of atoms to $N = 4 \times 10^5$, we improve the amount of conditional spin squeezing to $S^{-1} = 59(8)$ or 17.7(6) dB. The experimental measurement sequence is the same, but to avoid added noise from the π pulses, we only consider the reduction in the noise of the difference of two population measurements of the same spin state $R = [\Delta(N_{\downarrow f} - N_{\downarrow p})]/\Delta N_{\downarrow \mathrm{QPN}}]^2$ [Fig. 3(a)]. The information gained from the first measurement $N_{\uparrow p}$ is not used here, but its presence serves to spin echo away probe-induced inhomogeneous light shifts at the end of the

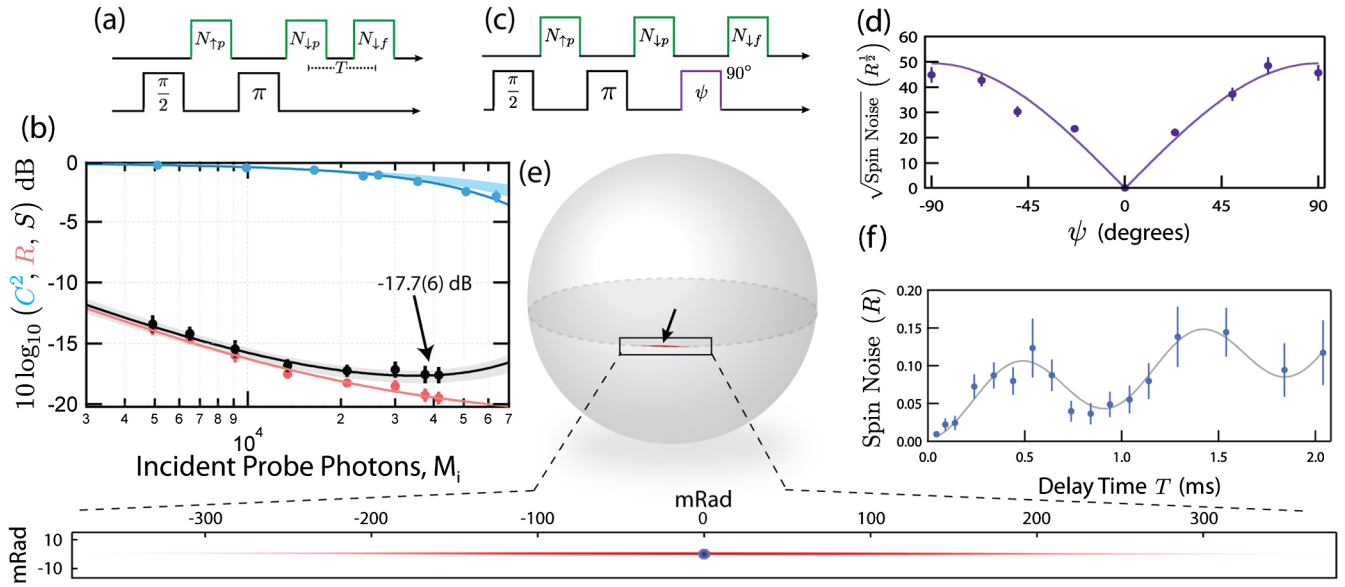

FIG. 3. (a) Experimental sequence for conditional spin squeezing, with labeling mirroring that of Fig. 2(a). (b) The squared contrast C^2 (blue), spin noise R (red), and spin squeezing S (black) are plotted versus the average number of incident photons M_i in a single measurement window. The solid lines are fits, the blue band is the predicted loss of contrast from free-space scattering, and the gray band indicates the total squeezing error bar. (c) The experimental sequence used to observe the backaction spin projection. (d) The measured spin noise R is plotted versus ψ with a fit (purple). (e) The reconstructed conditional probability distribution of the quantum state (red) on a Bloch sphere with the Bloch (black) vector. The distribution is magnified with a 1:1 aspect ratio and plotted with the equivalent coherent spin state (blue) in the lower panel. (f) Thermal radial motion of the atoms causes the spin noise R to oscillate at twice the radial trap frequency as the time separation T between the premeasurement and final measurement is increased.

premeasurement pair $N_{\uparrow p}$ and $N_{\downarrow p}$. Because the Bloch vector lies at the equator, small angular displacements of the polar angle could be sensed from changes in a single spin state's population alone.

In Fig. 3(b), we show the noise reduction R versus the average number of photons M_i incident upon the cavity during a single probe measurement window. Again, this is the directly observed noise reduction with no background subtractions or removal of noise of the final measurement applied. The maximum quantum noise reduction is $R^{-1} = 92(9)$, or 19.6(4) dB below the QPN, and is limited by both a technical noise floor 25 dB below the QPN and optomechanical effects induced by the probe light being turned on and off, an effect that increases with M_i. Also apparent in Fig. 3(b), the atomic coherence or contrast (blue) after the premeasurement decreases with increasing M_i due primarily to undesired free space scattering causing collapse of the individual atoms' wave functions into spin up (blue prediction band). The background contrast C_{BG} is obtained from a measurement with $M_i = 0$ in the two premeasurement windows. The black data and fit in Fig. 3(b) display the squeezing obtained by combining the reduction in noise with the reduction in contrast.

We also examine the backaction or antisqueezed spin projection. The experimental sequence is shown in Fig. 3(c) and is distinguished by the replacement of the rotation θ_{fb} with a microwave rotation about an axis parallel to the Bloch vector through a fixed angle ψ. Figure 3(d) shows the increase in spin noise R moving from the 17 dB squeezed (at $\psi = 0$) to antisqueezed (at $\psi = \pm 90°$) projections. Using an inverse Radon transform, we construct a visualization of the equivalent squeezed state, shown in Fig. 3(e). The original coherent state noise is shown in blue. The state has $\Delta J_z \Delta J_x / (\Delta J_{z,\mathrm{QPN}})^2 = 6.1 > 1$ and is no longer a minimum uncertainty state owing to the finite quantum efficiency for detecting the probe light. From the increase in area and its scaling with M_i we can infer the quantum efficiency of a joint measurement of a single population is $\tilde{Q}_1 = 38(14)\%$, in good agreement with an independent prediction of 37 (5)% from measuring path efficiencies, cavity loss, detector efficiencies, technical noise floors, and laser turn-on times (see the Supplemental Material [5]). Here, the total quantum efficiency of the full measurement sequence ($N_{\uparrow p}$, $N_{\downarrow p}$, $N_{\downarrow f}$) is effectively 4 times lower than $\tilde{Q}_1$ due to the additional noise in the final measurement $N_{\downarrow f}$ and the presently unused premeasurement $N_{\uparrow p}$.

In Fig. 3(f), we evaluate how well the conditional noise reduction can be maintained over a variable evolution time T. This is an important consideration for implementing conditional squeezing in atomic sensors. The contribution to R from technical noise sources is partially removed by performing the measurement sequence of Fig. 3(a) with no atoms present and subtracting the measured noise variance from the noise variances obtained with atoms present. The spin noise R is seen to oscillate at twice the radial frequency of the trapping potential due to thermal radial atomic motion that causes an oscillation in each atom's coupling to the cavity mode. The additional monotonic increase in R is not currently understood. A 3D optical lattice or a smaller atomic temperature to lattice depth ratio can be used to reduce the noise oscillations in the future.

The improved squeezing relative to previous work [25,44] was achieved by increasing the net quantum efficiency for probe detection from 5% to 37% (by constructing a single-ended cavity, reducing losses on cavity mirrors, and using homodyne detection), increasing the cavity finesse by 3.5, and implementing a two-probe laser technique that reduced the relative frequency noise between the probe laser and the empty cavity from 16 to 25 dB relative to the projection noise [45]. See the Supplemental Material [5].

It is physically reasonable to expect that the majority of the atoms participate in a single multipartite entangled state. The entanglement depth, or we believe more appropriately the "entanglement breadth" ζ, quantifies the minimum number of atoms that provably participate in a multipartite entangled state, no matter how weakly [46,47]. We find the largest breadth $\zeta = 400(120)$ atoms at squeezing $S^{-1} = 15$ dB, but at the largest squeezing we find $\zeta = 170(30)$ atoms.

Applying real-time feedback based on the outcome of joint measurements may allow for new applications in both quantum information technology and precision measurement. For instance, the utility of highly spin-squeezed states suffers from the fact that the state lives on a sphere, causing the backaction spin projection to couple into the measured spin projection J_z if the state is rotated too far from the equator. In clock applications, this results in needing to reduce the Ramsey phase evolution time such that the net enhancement in clock precision is far from approaching the Heisenberg limit [48]. It was recently proposed that joint measurement and feedback similar to that used here would allow one to actively measure and steer the backaction noise out of the measured spin projection and would thus allow enhancements in precision approaching the Heisenberg limit [31]. With improved atom-cavity coupling (e.g., higher finesse and smaller mode waist size), even greater amounts of squeezing than that reported here can be achieved in principle [42]. However, it will be critical to consider current limiting effects such as optomechanical ringing and time-varying couplings between measurements due to atomic motion in order to achieve significant improvements. Having now shown that large enhancements in phase resolution using entanglement are achievable in real systems that are compatible with state-of-the-art precision measurements, the next steps may include application to matter-wave interferometers [32] and optical lattice clocks [28].

We thank Elissa Picozzi for construction of the homodyne detector and Matthew A. Norcia for helpful discussions. This work is supported by NIST, DARPA QuASAR,

ARO, and by the National Science Foundation under Grant No. 1125844. K. C. C. acknowledges support from the NDSEG fellowship.

[1] W. M. Itano, J. C. Bergquist, J. J. Bollinger, J. M. Gilligan, D. J. Heinzen, F. L. Moore, M. G. Raizen, and D. J. Wineland, Phys. Rev. A **47**, 3554 (1993).
[2] D. J. Wineland, J. J. Bollinger, W. M. Itano, F. L. Moore, and D. J. Heinzen, Phys. Rev. A **46**, R6797 (1992).
[3] M. Kitagawa and M. Ueda, Phys. Rev. A **47**, 5138 (1993).
[4] O. Hosten, N. J. Engelsen, R. Krishnakumar,and M. A. Kasevich, Nature (London) **529**, 505 (2016).
[5] See Supplemental Material at http://link.aps.org/supplemental/10.1103/PhysRevLett.116.093602, which includes Refs. [6–8], for additional details about the experimental system and methods, emphasizing improvements beyond previous work.
[6] D. J. Wineland, J. J. Bollinger, W. M. Itano, and D. J. Heinzen, Phys. Rev. A **50**, 67 (1994).
[7] U. Leonhardt, *Measuring the Quantum State of Light*, Cambridge Studies in Modern Optics (Cambridge University Press, Cambridge, England, 1997).
[8] Z. Chen, J. G. Bohnet, J. M. Weiner, and J. K. Thompson, Rev. Sci. Instrum. **83**, 044701 (2012).
[9] C. A. Sackett, D. Kielpinski, B. E. King, C. Langer, V. Meyer, C. J. Myatt, M. Rowe, Q. A. Turchette, W. M. Itano, D. J. Wineland, and C. Monroe, Nature (London) **404**, 256 (2000).
[10] D. Leibfried, E. Knill, S. Seidelin, J. Britton, R. B. Blakestad, J. Chiaverini, D. B. Hume, W. M. Itano, J. D. Jost, C. Langer, R. Ozeri, R. Reichle, and D. J. Wineland, Nature (London) **438**, 639 (2005).
[11] T. Monz, P. Schindler, J. T. Barreiro, M. Chwalla, D. Nigg, W. A. Coish, M. Harlander, W. Hänsel, M. Hennrich, and R. Blatt, Phys. Rev. Lett. **106**, 130506 (2011).
[12] A. Noguchi, K. Toyoda, and S. Urabe, Phys. Rev. Lett. **109**, 260502 (2012).
[13] B. Lücke, J. Peise, G. Vitagliano, J. Arlt, L. Santos, G. Tóth, and C. Klempt, Phys. Rev. Lett. **112**, 155304 (2014).
[14] M. F. Riedel, P. Böhi, Y. Li, T. W. Hänsch, A. Sinatra, and P. Treutlein, Nature (London) **464**, 1170 (2010).
[15] C. D. Hamley, C. S. Gerving, T. M. Hoang, E. M. Bookjans, and M. S. Chapman, Nat. Phys. **8**, 305 (2012).
[16] W. Muessel, H. Strobel, D. Linnemann, D. B. Hume, and M. K. Oberthaler, Phys. Rev. Lett. **113**, 103004 (2014).
[17] R. Bücker, J. Grond, S. Manz, T. Berrada, T. Betz, C. Koller, U. Hohenester, T. Schumm, A. Perrin, and J. Schmiedmayer, Nat. Phys. **7**, 608 (2011).
[18] I. D. Leroux, M. H. Schleier-Smith, and V. Vuletić, Phys. Rev. Lett. **104**, 073602 (2010).
[19] A. Kuzmich, N. P. Bigelow, and L. Mandel, Europhys. Lett. **42**, 481 (1998).
[20] J. Appel, P. J. Windpassinger, D. Oblak, U. B. Hoff, N. Kjærgaard, and E. S. Polzik, Proc. Natl. Acad. Sci. U.S. A. **106**, 10960 (2009).
[21] M. H. Schleier-Smith, I. D. Leroux, and V. Vuletić, Phys. Rev. Lett. **104**, 073604 (2010).
[22] W. Wasilewski, K. Jensen, H. Krauter, J. J. Renema, M. V. Balabas, and E. S. Polzik, Phys. Rev. Lett. **104**, 133601 (2010).
[23] I. D. Leroux, M. H. Schleier-Smith, and V. Vuletić, Phys. Rev. Lett. **104**, 250801 (2010).
[24] Z. Chen, J. G. Bohnet, S. R. Sankar, J. Dai, and J. K. Thompson, Phys. Rev. Lett. **106**, 133601 (2011).
[25] J. G. Bohnet, K. C. Cox, M. A. Norcia, J. M. Weiner, Z. Chen, and J. K. Thompson, Nat. Photonics **8**, 731 (2014).
[26] N. Behbood, F. Martin Ciurana, G. Colangelo, M. Napolitano, G. Tóth, R. J. Sewell, and M. W. Mitchell, Phys. Rev. Lett. **113**, 093601 (2014).
[27] R. J. Sewell, M. Koschorreck, M. Napolitano, B. Dubost, N. Behbood, and M. W. Mitchell, Phys. Rev. Lett. **109**, 253605 (2012).
[28] M. A. Norcia and J. K. Thompson, arXiv:1506.02297.
[29] D. Riste, M. Dukalski, C. A. Watson, G. de Lange, M. J. Tiggelman, Y. M. Blanter, K. W. Lehnert, R. N. Schouten, and L. DiCarlo, Nature (London) **502**, 350 (2013).
[30] N. Roch, M. E. Schwartz, F. Motzoi, C. Macklin, R. Vijay, A. W. Eddins, A. N. Korotkov, K. B. Whaley, M. Sarovar, and I. Siddiqi, Phys. Rev. Lett. **112**, 170501 (2014).
[31] J. Borregaard and A. S. Sørensen, Phys. Rev. Lett. **111**, 090801 (2013).
[32] J. Esteve, C. Gross, A. Weller, S. Giovanazzi, and M. K. Oberthaler, Nature (London) **455**, 1216 (2008).
[33] G.-B. Jo, Y. Shin, S. Will, T. A. Pasquini, M. Saba, W. Ketterle, D. E. Pritchard, M. Vengalattore, and M. Prentiss, Phys. Rev. Lett. **98**, 030407 (2007).
[34] J. F. Sherson, H. Krauter, R. K. Olsson, B. Julsgaard, K. Hammerer, I. Cirac, and E. S. Polzik, Nature (London) **443**, 557 (2006).
[35] H. Krauter, D. Salart, C. A. Muschik, J. M. Petersen, H. Shen, T. Fernholz, and E. S. Polzik, Nat. Phys. **9**, 400 (2013).
[36] D. Nigg, M. Müller, E. A. Martinez, P. Schindler, M. Hennrich, T. Monz, M. A. Martin-Delgado, and R. Blatt, Science **345**, 302 (2014).
[37] B. Vlastakis, G. Kirchmair, Z. Leghtas, S. E. Nigg, L. Frunzio, S. M. Girvin, M. Mirrahimi, M. H. Devoret, and R. J. Schoelkopf, Science **342**, 607 (2013).
[38] L. K. Thomsen, S. Mancini, and H. M. Wiseman, Phys. Rev. A **65**, 061801 (2002).
[39] L. K. Thomsen, S. Mancini, and H. M. Wiseman, J. Phys. B **35**, 4937 (2002).
[40] R. Inoue, Shin-Ichi-Ro Tanaka, R. Namiki, T. Sagawa, and Y. Takahashi, Phys. Rev. Lett. **110**, 163602 (2013).
[41] A. Sørensen, L.-M. Duan, J. I. Cirac, and P. Zoller, Nature (London) **409**, 63 (2001).
[42] Z. Chen, J. G. Bohnet, J. M. Weiner, K. C. Cox, and J. K. Thompson, Phys. Rev. A **89**, 043837 (2014).
[43] J. Hu, W. Chen, Z. Vendeiro, H. Zhang, and V. Vuletić, arXiv:1510.01021.
[44] K. C. Cox, M. A. Norcia, J. M. Weiner, J. G. Bohnet, and J. K. Thompson, Appl. Phys. Lett. **105**, 261102 (2014).
[45] K. C. Cox, J. M. Weiner, G. P. Greve, and J. K. Thompson, in *Frequency Control Symposium the European Frequency and Time Forum (FCS), 2015 Joint Conference of the IEEE International* (IEEE, New York, 2015), pp. 351–356.
[46] A. S. Sørensen and K. Mølmer, Phys. Rev. Lett. **86**, 4431 (2001).
[47] R. McConnell, H. Zhang, J. Hu, S. Cuk, and V. Vuletic, Nature (London) **519**, 439 (2015).
[48] A. André, A. S. Sørensen, and M. D. Lukin, Phys. Rev. Lett. **92**, 230801 (2004).